

The Application of Constricted Variational Density Functional Theory to Excitations Involving Electron Transitions from Occupied Lone-Pair Orbitals to Virtual π^* Orbitals

Tom Ziegler,^{*,†} Mykhaylo Krykunov,[†] and John Cullen[‡]

[†]Department of Chemistry, University of Calgary, University Drive 2500, Calgary AB T2N-1N4, Canada

[‡]Department of Chemistry, University of Manitoba, Winnipeg MB, R3T-2N2, Canada

 Supporting Information

ABSTRACT: We have applied the constricted variational density functional method (CV(*n*)-DFT) to $n \rightarrow \pi^*$ transitions in which an electron is moved from an occupied lone-pair orbital n to a virtual π^* orbital. A total of 34 transitions involving 16 different compounds were considered using the local density approximation (LDA), Becke, three-parameter, Lee–Yang–Parr (B3LYP), and BHLYP functionals. The DFT-based results were compared to the “best estimates” (BE) from high-level ab initio calculations. With energy terms included to second order in the variational parameters (CV(2)-DFT), our theory is equivalent to the adiabatic version of time-dependent density functional theory (DFT). We find that calculated excitation energies for CV(2)-DFT using LDA and BHLYP differ substantially from BE with root-mean-square-deviations (rmsd) of 0.86 and 0.69 eV, respectively, whereas B3LYP affords an excellent fit with BE at rmsd = 0.18 eV. Resorting next to CV(∞)-DFT, where energy terms to all orders in the variational parameters are included, results in all three functionals in too high excitation energies with rmsd = 1.69, 1.14, and 0.93 eV for LDA, B3LYP, and BHLYP, respectively. Adding in orbital relaxation considerably improves the results with rmsd = 0.54, 0.30, and 0.48 eV for LDA, B3LYP, and BHLYP, respectively. It is concluded that CV(∞)-DFT with orbital relaxation is a robust method for which the accuracy is less functionally dependent than that of CV(2)-DFT or adiabatic TDDFT.

1. INTRODUCTION

Time-dependent DFT (TDDFT) in its adiabatic formulation^{1–7} has emerged as an efficient tool for the study of excited states. Extensive benchmarking of adiabatic TDDFT^{8–12} has revealed that the calculated excitation energies are in fair agreement with experiment. It is thus to be expected that adiabatic TD-DFT will be used increasingly as a reasonable compromise between accuracy and computational cost in many applications.^{8–12} However, the extensive benchmarking has revealed some systematic errors^{8–14} in the calculated excitation energies when use is made of the generalized gradient approximation (GGA) as well as the popular approximate hybrid functionals containing fractions of exact Hartree–Fock exchange. The largest deviations^{8–14} are found for transitions where electrons are moved between two separated regions of space [charge-transfer (CT) transitions] or between orbitals of different spatial extent (Rydberg transitions).^{10–14}

We have in some recent studies^{15–18} analyzed the reason for the deviations between experimental CT excitation energies and estimates obtained from TDDFT applications. It was found that the deviations for a large part can be traced back to the simple approach taken in standard TDDFT, where terms depending on the linear orbital response parameter set U only are kept to second order in U for the energy expression.^{15–18} While this simple linear response approach is adequate for the corresponding Hartree–Fock time-dependent formulation where self-interaction is absent,¹⁷ it is inadequate for TDDFT applied to most approximate functionals where self-interaction terms are present.^{15–18} In those cases, higher-order terms in U must be included into the energy expression.^{15–18}

With the intention of including higher-order terms, we have developed a constricted variational density functional approach (CV(*n*)-DFT) to the calculation of excitation energies and excited-state properties.^{18–20} In its second-order formulation (CV(2)-DFT) this theory coincides with adiabatic TD-DFT when use is made of the popular Tamm–Dancoff approximation²¹ within both theories. However, in the general formulation of CV(*n*)-DFT terms to any order in U^n are included.

The objective of the current study is to consider another category of excitations in addition to CT where electrons are moved between orbitals of different spatial extent, namely the $n \rightarrow \pi^*$ transitions. In this case an electron is excited from an in-plane doubly occupied lone-pair orbital n to a π^* orbital situated perpendicular to the molecular plane. Obviously there will be only a modest overlap between the densities of n and π^* , although it might be larger than the overlaps for the densities of π_A and π_B^* in the CT transition $\pi_A \rightarrow \pi_B^*$, where A and B might be several angstroms apart.

We shall in the present study apply the pure LDA²² functional as well as the hybrids²³ B3LYP and BHLYP to the $n \rightarrow \pi^*$ transitions. As these transitions in all the considered cases turned out to be true one-orbital transitions where an electron is transferred from $n \rightarrow \pi^*$, we shall also make use of the self-consistent field Δ SCF scheme,²⁴ where one carries out Kohn–Sham SCF calculations on the $(n)^2$ and $n\pi^*$ configurations. For the simple one-orbital $n \rightarrow \pi^*$ transitions studied here the Δ SCF

Received: April 15, 2011

Published: June 28, 2011

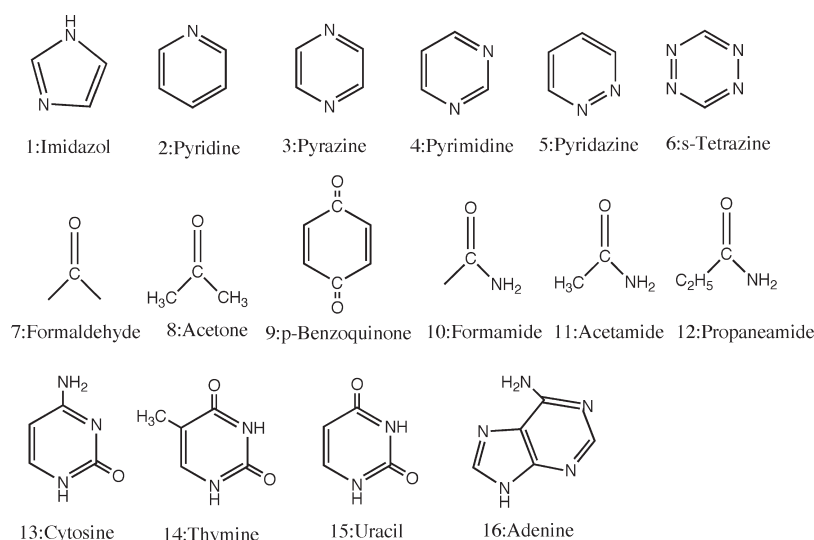


Figure 1. Molecules investigated in this study.

scheme can be considered as equivalent to the SCF-CV(∞)-DFT method²⁰ discussed in Section 3. We shall compare our calculated DFT-based excitation energies to those obtained in a recent benchmark study by Schreiber¹⁰ et al. based on high level ab initio methods¹⁰ and termed “best estimates” (BE) by the authors. The 16 molecules investigated here are shown in Figure 1.

2. COMPUTATIONAL DETAILS

All calculations were based on DFT as implemented in the ADF program version 2010.²⁵ Our calculations employed a standard triple- ζ Slater-type orbital (STO) basis with one set of polarization functions for all atoms.²⁶ Use was made of the local density approximation in the Vosko, Wilk, and Nusair (VWN) parameterization²² as well as the B3LYP and B97LYP hybrid functionals by Becke.²³ All electrons were considered as valence. The parameter (ACINT) for the precision of the numerical integration was set to 5.0. Use was made of a special auxiliary STO basis to fit the electron density in each cycle for an accurate representation of the exchange and the Coulomb potentials. All CV(2)-DFT¹⁸ and CV(∞)-DFT²⁰ calculations were carried out with a developers version of ADF-2010. The Cartesian coordinates of the 16 benchmark molecules shown in Figure 1 were taken from the Supporting Information of ref 10. The ground-state geometries of these molecules were optimized at the MP2/6-31G* level of theory.¹⁰

3. CV(N)-DFT

We have recently introduced a variational approach based on density functional theory for the description of excited states.^{18,20} In CV(n)-DFT we carry out a unitary transformation²⁰ among occupied $\{\varphi_i; i = 1, \text{occ}\}$ and virtual $\{\varphi_a; a = 1, \text{vir}\}$ ground-state orbitals:

$$Y \begin{pmatrix} \varphi_{\text{occ}} \\ \varphi_{\text{vir}} \end{pmatrix} = e^U \begin{pmatrix} \varphi_{\text{occ}} \\ \varphi_{\text{vir}} \end{pmatrix} = \left(\sum_{n=0}^{\infty} \frac{(U^2)^n}{2n!} \right) \begin{pmatrix} \varphi_{\text{occ}} \\ \varphi_{\text{vir}} \end{pmatrix} = \begin{pmatrix} \varphi'_{\text{occ}} \\ \varphi'_{\text{vir}} \end{pmatrix} \quad (1)$$

Here φ_{occ} and φ_{vir} are concatenated column vectors containing the sets $\{\varphi_i; i = 1, \text{occ}\}$ and $\{\varphi_a; a = 1, \text{vir}\}$, whereas φ'_{occ} and φ'_{vir}

are concatenated column vectors containing the resulting sets $\{\varphi'_i; i = 1, \text{occ}\}$ and $\{\varphi'_a; a = 1, \text{vir}\}$ of occupied and virtual excited-state orbitals, respectively. The unitary transformation matrix Y is in eq 1 expressed in terms of a skew symmetric matrix U as

$$Y = e^U = I + U + \frac{U^2}{2} + \cdots = \sum_{n=0}^{\infty} \frac{U^n}{n!} = \sum_{n=0}^{\infty} \frac{(U^2)^n}{2n!} + U \sum_{n=0}^{\infty} \frac{(U^2)^n}{(2n+1)!} \quad (2)$$

Here $U_{ij} = U_{ab} = 0$ where “ ij ” refer to the occupied set $\{\varphi_i; i = 1, \text{occ}\}$, whereas “ ab ” refer to $\{\varphi_a; a = 1, \text{vir}\}$. Further, U_{ai} is the variational mixing matrix elements that combines virtual and occupied ground-state orbitals in the excited state with $U_{ai} = -U_{ia}$. Thus, the entire matrix U is made up of $\text{occ} \times \text{vir}$ independent elements U_{ai} that also can be organized in the column vector \vec{U} . For a given U we can, with the help of eq 2, generate a set of “occupied” excited-state orbitals:

$$\varphi'_i = \sum_p^{\text{occ} + \text{vir}} Y_{pi} \varphi_p = \sum_j^{\text{occ}} Y_{ji} \varphi_j + \sum_a^{\text{vir}} Y_{ai} \varphi_a \quad (3)$$

that are orthonormal to any order in U_{ai} .

In the simple CV(2)-DFT theory,¹⁸ the unitary transformation of eq 2 is carried out to second order in U . We thus obtain the occupied excited-state orbitals to the second order as

$$\varphi'_i = \varphi_i + \sum_a^{\text{vir}} U_{ai} \varphi_a - \frac{1}{2} \sum_j^{\text{occ}} \sum_a^{\text{vir}} U_{ai} U_{aj} \varphi_j \quad (4)$$

from which we can generate the excited state Kohn–Sham density matrix to the second order as

$$\begin{aligned} \rho'(1, 1') &= \rho^{(0)}(1, 1') + \Delta\rho'(1, 1') = \rho^{(0)}(1, 1') \\ &+ \sum_i^{\text{occ}} \sum_a^{\text{vir}} U_{ai} \varphi_a(1') \varphi_i^*(1) + \sum_i^{\text{occ}} \sum_a^{\text{vir}} U_{ai}^* \varphi_a^*(1) \varphi_i(1') \\ &+ \sum_i^{\text{occ}} \sum_a^{\text{vir}} \sum_b^{\text{vir}} U_{ai}^* U_{bi} \varphi_a(1') \varphi_b^*(1) \\ &- \sum_i^{\text{occ}} \sum_j^{\text{occ}} \sum_a^{\text{vir}} U_{ai} U_{aj}^* \varphi_i(1') \varphi_j^*(1) \end{aligned} \quad (5)$$

Next the expression for $\rho'(1,1')$ makes it possible to write down the corresponding excited state Kohn–Sham energy to the second order as

$$E_{KS}[\rho'(1,1')] = E_{KS}[\rho^0] + \sum_{ai} U_{ai} U_{ai}^* (\varepsilon_a^0 - \varepsilon_i^0) + \sum_{ai} \sum_{bj} U_{ai} U_{bj}^* K_{ai,bj} + \frac{1}{2} \sum_{ai} \sum_{bj} U_{ai} U_{bj} K_{ai,jb} + \frac{1}{2} \sum_{ai} \sum_{bj} U_{ai}^* U_{bj}^* K_{ai,jb} + O[U^{(3)}] \quad (6)$$

Here $E_{KS}[\rho^0]$ is the ground-state energy and “ a,b ” run over virtual ground-state canonical orbitals, whereas “ i,j ” run over occupied ground-state canonical orbitals. Further

$$K_{nu,tq} = K_{nu,tq}^C + K_{nu,tq}^{XC} \quad (7)$$

where

$$K_{nu,tq}^C = \int \int \varphi_r^*(1) \varphi_u(1) \frac{1}{r_{12}} \varphi_t^*(2) \varphi_q(2) dv_1 dv_2 \quad (8)$$

whereas

$$K_{nu,tq}^{XC(HF)} = - \int \int \varphi_r^*(1) \varphi_q(1) \frac{1}{r_{12}} \varphi_t^*(2) \varphi_u(2) dv_1 dv_2 \quad (9)$$

for Hartree–Fock exchange correlation and

$$K_{nu,tq}^{XC(DFT)} = \delta(m_{sr}, m_{su}) \delta(m_{st}, m_{sq}) \int \varphi_r^*(\vec{r}_1) \varphi_u(\vec{r}_1) \times [f^{(m_{sr}, m_{st})}(\rho^0)] \varphi_t^*(\vec{r}_1) \varphi_q(\vec{r}_1) d\vec{r}_1 \quad (10)$$

for DFT exchange correlation. In eq 10 $m_{sr} = 1/2$ for a spin orbital $\varphi_r(1)$ of α -spin, whereas $m_{sr} = -1/2$ for a spin orbital $\varphi_r(1)$ of β -spin. In addition the kernel $f^{(\tau,v)}(\rho^0)$ is the second functional derivative of E_{XC} with respect to ρ_α and ρ_β :

$$f^{\tau,v}(\rho_\alpha^0, \rho_\beta^0) = \left(\frac{\partial^2 E_{XC}}{\partial \rho_\tau \partial \rho_v} \right)_0 \quad \tau = \alpha, \beta; \quad v = \alpha, \beta \quad (11)$$

Finally ε_i^0 and ε_a^0 in eq 6 are the ground-state orbital energies of respectively $\varphi_i(1)$ and $\varphi_a(1)$.

In CV(2)-DFT¹⁸ we seek points on the energy surface $E_{KS}[\rho']$ such that $\Delta E_{KS}[\Delta\rho'] = E_{KS}[\rho'] - E_{KS}[\rho^0]$ represents a transition energy. Obviously, a direct optimization of $\Delta E_{KS}[\Delta\rho']$ without constraints will result in $\Delta E_{KS}[\Delta\rho'] = 0$ and $U = 0$. We¹⁸ now introduce the constraint that the electron excitation must represent a change in density $\Delta\rho'$, where one electron in eq 5 is transferred from the occupied space represented by $\Delta\rho_{occ} = -\sum_{ija} U_{ai} U_{aj}^* \varphi_i(1') \varphi_j^*(1)$ to the virtual space represented by $\Delta\rho_{vir} = \sum_{iab} U_{ai} U_{bi}^* \varphi_a(1') \varphi_b^*(1)$. An integration of $\Delta\rho_{occ}$ and $\Delta\rho_{vir}$ over all space affords $-\Delta q_{occ} = \Delta q_{vir} = \sum_{ai} U_{ai} U_{ai}^*$. We shall thus introduce the constraint $\sum_{ai} U_{ai} U_{ai}^* = 1$. Constructing next the Lagrangian $L = E_{KS}[\rho'] + \lambda(1 - \sum_{ai} U_{ai} U_{ai}^*)$ with λ being a Lagrange multiplier and demanding that L be stationary to any real variation in U results in the eigenvalue equation:

$$(A^{KS} + B^{KS}) \vec{U}^{(I)} = \lambda_{(I)} \vec{U}^{(I)} \quad (12)$$

where

$$A_{ai,bj}^{KS} = \delta_{ab} \delta_{ij} (\varepsilon_a^0 - \varepsilon_i^0) + K_{ai,bj}^{KS}; \quad B_{ai,bj}^{KS} = K_{ai,jb}^{KS} \quad (13)$$

We can now from eq 12 determine the sets of mixing coefficients $\{\vec{U}^{(I)}; I = 1, \text{occ} \times \text{vir}\}$ that make L stationary and represent excited states. The corresponding excitation energies are given by

$\lambda_{(I)}$, as it can be seen by substituting $\vec{U}^{(I)}$ into eq 6 and making use of the constraint and normalization condition $\vec{U}^{(I)+} \vec{U}^{(I)} = 1$ after multiplying on both sides with $\vec{U}^{(I)+}$.

Within the Tamm–Dancoff approximation²¹ eq 12 reduces to

$$A^{KS} \vec{U}^{(I)} = \lambda_{(I)} \vec{U}^{(I)} \quad (14)$$

which is identical in form to the equation one obtains from TDDFT in its adiabatic formulation^{1–6} after applying the same Tamm–Dancoff²¹ approximation.

Having determined $\vec{U}^{(I)}$ from either eq 12 or 14 allows us²⁰ now to carry out the unitary transformation of eq 1 to all orders. The resulting occupied excited-state orbitals are given by²⁰

$$\phi_j' = \cos[\eta\gamma_j] \phi_j^o + \sin[\eta\gamma_j] \phi_j^v; \quad j = 1, \text{occ} \quad (15)$$

here ϕ_j^o and ϕ_j^v are according to the corresponding orbital theory of Hall and Amos²⁷ eigenvectors to, respectively, D_{occ} and D_{vir} with the same eigenvalues γ_i where $(D_{\text{occ}}^2)_{ij} = \sum_a^{\text{vir}} U_{ai} U_{aj}$ and $(D_{\text{vir}}^2)_{ab} = \sum_i^{\text{occ}} U_{ai} U_{bi}$. Here ϕ_j^o is a linear combination of occupied ground-state orbitals, whereas ϕ_j^v is a linear combinations of virtual ground-state orbitals. Thus in the corresponding orbital representation²⁷ only one occupied orbital ϕ_j^o mixes with one corresponding virtual orbital ϕ_j^v for each occupied excited-state orbital ϕ_j' when the unitary transformation is carried out to all orders according to eq 1. Martin²⁸ has used the representation of corresponding orbitals to analyze excitations described by TDDFT and TDHF. In his interesting analysis $\{\phi_j^o(1), \phi_j^v(1)\}$ are referred to as natural transition orbitals (NTO).

The change in the density matrix $\Delta\rho^{(\infty)}$ due to a one-electron excitation takes on the compact form of

$$\Delta\rho^{(\infty)}(1,1') = \sum_j^{\text{occ}} \sin^2[\eta\gamma_j] [\phi_j^v(1') \phi_j^v(1) - \phi_j^o(1') \phi_j^o(1)] + \sum_j^{\text{occ}} \sin[\eta\gamma_j] \cos[\eta\gamma_j] [\phi_j^v(1) \phi_j^o(1') + \phi_j^v(1') \phi_j^o(1)] \quad (16)$$

when the unitary transformation in eq 1 is carried out to all orders. In eqs 15 and 16 the scaling factor η is introduced to ensure that $\Delta\rho^{(\infty)}(1,1')$ represents the transfer of a single electron from the occupied orbital space density, $\sin^2[\eta\gamma_j] \phi_j^o(1') \phi_j^o(1)$ to the virtual orbital space density $\sum_j^{\text{occ}} \sin^2[\eta\gamma_j] \phi_j^v(1') \phi_j^v(1)$ or

$$\sum_j^{\text{occ}} \sin^2[\eta\gamma_j] = 1 \quad (17)$$

Here the constraint of eq 17 is a generalization of the corresponding second-order constraint $\sum_{ai} U_{ai} U_{ai}^* = 1$ used to derive eqs 13 and 14.

We finally get for the excitation energy including terms to all orders in U :

$$\Delta E^{(\infty)} = E_{KS}^{(\infty)}[\rho^0 + \Delta\rho^{(\infty)}] - E_{KS}[\rho^0] = - \sum_j^{\text{occ}} \sin^2[\eta\gamma_j] F_{j,j}^{KS}[\rho^0 + \frac{1}{2} \Delta\rho^{(\infty)}] + \sum_j^{\text{occ}} \sin^2[\eta\gamma_j] F_{j,j}^{KS}[\rho^0 + \frac{1}{2} \Delta\rho^{(\infty)}] + \sum_j^{\text{occ}} \cos[\eta\gamma_j] \sin[\eta\gamma_j] F_{j,j}^{KS} \left[\rho^0 + \frac{1}{2} \Delta\rho^{(\infty)} \right] + \sum_j^{\text{occ}} \cos[\eta\gamma_j] \sin[\eta\gamma_j] F_{j,j}^{KS} \left[\rho^0 + \frac{1}{2} \Delta\rho^{(\infty)} \right] + O^{[3]}(\Delta\rho^{(\infty)}) \quad (18)$$

Here eq 18 is derived by Taylor expanding²⁹ $E_{KS}^{(\infty)}[\rho^0 + \Delta\rho^{(\infty)}]$ and $E_{KS}[\rho^0]$ from the common intermediate density $\rho^0 + 1/2 \Delta\rho^{(\infty)}$. Further, $F^{KS}[\rho^0 + 1/2 \Delta\rho^{(\infty)}]$ is the Kohn–Sham Fock

Table 1. Vertical $n \rightarrow \pi^*$ Singlet Excitation Energies^a

molecule	state	best ^b	LDA(VWN)			B3LYP		
			CV(2) ^c	CV(∞) ^d	Δ SCF	CV(2) ^c	CV(∞) ^d	Δ SCF ^e
imidazole	A''	6.81	5.79	9.51	6.59	6.53	8.01	6.47
pyridine	B ₁	4.59	4.30	6.30	4.58	4.92	5.91	4.69
	A ₂	5.11	4.35	7.22	4.94	5.17	7.13	5.15
pyrazine	B _{3u}	3.95	3.52	3.68	3.45	4.09	3.94	3.85
	A _u	4.81	3.91	5.01	4.16	4.74	5.40	4.63
	B _{2g}	5.56	5.03	5.59	5.10	5.67	5.72	5.48
	B _{1g}	6.6	5.40	7.40	5.87	6.40	7.84	6.38
pyrimidine	B ₁	4.55	3.73	4.61	3.87	4.37	4.81	4.14
	A ₂	4.91	3.93	5.22	4.21	4.68	5.35	4.54
pyridazine	B ₁	3.78	3.10	4.63	3.29	3.74	4.38	3.55
	A ₂	4.31	3.41	5.49	3.84	4.26	5.62	4.15
	A ₂	5.77	4.97	5.78	5.06	5.55	5.80	5.35
s-tetrazine	B _{3u}	2.29	1.83	2.04	1.75	2.41	2.29	2.15
	A _u	3.51	2.73	3.58	2.95	3.59	3.98	3.49
	B _{1g}	4.73	4.01	4.27	3.91	4.88	4.72	4.56
	A _u	5.5	4.55	4.78	4.50	5.20	5.06	4.97
	B _{2g}	5.2	4.72	5.04	4.82	5.40	5.18	5.17
formaldehyde	A ₂	3.88	3.64	4.65	3.73	3.93	4.48	3.52
acetone	A ₂	4.4	4.16	5.44	4.33	4.41	5.11	4.02
p-benzoquinone	B _{1g}	2.76	1.86	2.18	1.88	2.54	2.55	2.40
	A _u	2.77	2.00	2.62	2.11	2.69	2.90	2.55
	B _{3u}	5.64	4.29	6.36	4.67	5.47	6.69	5.40
formamide	A''	5.63	5.33	7.23	5.66	5.58	6.75	5.28
acetamide	A''	5.69	5.31	7.33	5.67	5.59	6.84	5.31
propanamide	A''	5.72	5.34	7.30	5.67	5.60	6.82	5.34
cytosine	A''	4.87	3.74	10.04	4.64	4.78	7.49	4.83
	A''	5.26	4.41	7.89	5.12	5.17	7.19	
thymine	A''	4.82	4.04	6.95	4.57	4.74	6.64	5.59
	A''	6.16	4.75	9.07	6.06	5.83	8.43	6.15
uracil	A''	4.8	3.91	7.22	4.52	4.66	6.73	4.54
	A''	6.1	4.69	9.26	6.03	5.75	7.98	6.07
	A''	6.56	5.15	8.84	5.58	6.14	6.75	
adenine	A''	5.12	4.22	5.78	4.47	5.01	5.73	4.91
	A''	5.75	5.00	6.01	5.16	5.69	5.86	
rmsd($n \rightarrow \pi^*$)			0.86	1.69	0.54	0.18	1.14	0.30

^aIn eV. ^bTheoretical best estimates from ref 10. ^cCV(2)-DFT singlet transition energy from eq 19 where the Tamm–Dancoff approximation²¹ has been used. ^dCV(∞)-DFT singlet transition energy from eq 22. ^e Δ SCF^{24,30} excitation energies from eq 23.

operator defined with respect to the intermediate Kohn–Sham density matrix $\rho^0 + 1/2\Delta\rho^{(\infty)}$, whereas $F_{pq}^{KS}[\rho^0 + 1/2\Delta\rho^{(\infty)}]$ is a matrix element of this operator involving the two orbitals φ_p, φ_q . The expression in eq 18 is exact to the third order in $\Delta\rho^{(\infty)}$, which is usually enough.²⁹ However its accuracy can be extended to any desired order in $\Delta\rho^{(\infty)}$.²⁹

The energy expression in eq 18 is perturbative in the sense that we make use of a U matrix optimized with respect to the second-order energy expression of eq 6. We refer to this method as CV(∞)-DFT.²⁰ We might alternatively optimize U directly with respect to the energy expression of eq 18 in a self-consistent fashion. Such a procedure termed SCF-CV(∞)-DFT has been formulated²⁰ but not yet implemented. We shall in the present study of $n \rightarrow \pi^*$ transitions make use of the Δ SCF scheme^{24,30} which is equivalent to SCF-CV(∞)-DFT when, as in the current case, the excitation can be described by a single orbital transition.

4. RESULTS AND DISCUSSION

We sample in Table 1 the calculated $n \rightarrow \pi^*$ excitation energies based on LDA and B3LYP for 34 transitions. For each functional, results are given for CV(2)-DFT,¹⁸ CV(∞)-DFT,²⁰ and Δ SCF.^{24,30} We compare further the DFT-based results with

the “best estimate” by Schreiber¹⁰ et al. based on high-level ab initio wave function methods. Please note that the CV(2)-DFT results in Table 1 are identical to those based on TD-DFT after use has been made of the Tamm–Dancoff approximation.²¹

LDA. The LDA results compiled in Table 1 are also shown in Figure 2 where we plot the calculated excitation energies due to CV(2)-DFT, CV(∞)-DFT and Δ SCF relative to BE.¹⁰

In the single orbital transition $n \rightarrow \pi^*$ we can represent the resulting singlet excited states as $\Psi_{n \rightarrow \pi^*}^S = 1/(2)^{1/2} [|n\pi^*| + |\pi^*n|]$. In adiabatic TDDFT or CV(2)-DFT the corresponding singlet transition energy is given by^{2,15}

$$\Delta E_S^{(2)} = \varepsilon_{\pi^*} - \varepsilon_n + 2K_{n\pi^*, n\pi^*} - K_{n\pi^*, \pi^*n} \quad (19)$$

within the Tamm–Dancoff²¹ approximation.

We see from Figure 1 where we plot $\Delta E_S^{(2)}$ relative to BE¹⁰ that LDA systematically underestimates the excitation energies at the CV(2)-DFT level with a rmsd of 0.86 eV, see Table 1. This can be attributed to the fact that the highest occupied molecular orbital–lowest unoccupied molecular orbital (HOMO–LUMO) gap $\varepsilon_{\pi^*} - \varepsilon_n$ for pure functionals typically is much smaller than the HOMO to LUMO excitation energy. Further, $K_{n\pi^*, n\pi^*}$, $K_{n\pi^*, \pi^*n}$ although positive are rather small, since n and π^* are in different

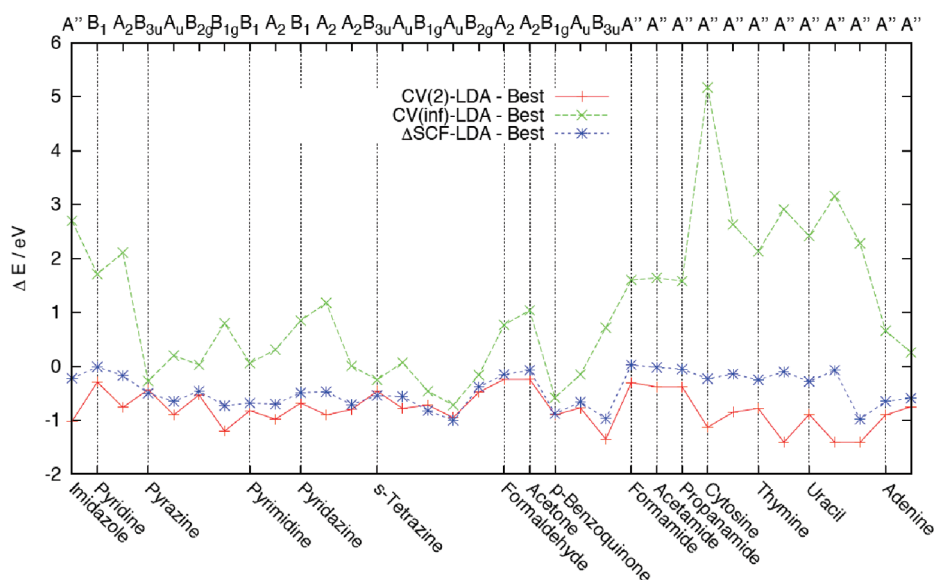


Figure 2. Difference between CV(2)-LDA, CV(∞)-LDA, ΔSCF-LDA, and best estimate¹⁰.

regions. The situation is quite similar to that of the $\pi_A \rightarrow \pi_B^*$ CT transitions, where pure functionals also underestimate the excitation energies at the CV(2)-DFT level.¹⁵ In that case the underestimation is even larger as $K_{\pi_A \pi_B^*, \pi_A \pi_B^*}$ is negligible due to the physical separation of A and B.

Turning next to the CV(∞)-DFT level of theory, we have in the case of the single orbital transition $n_G \rightarrow \pi^*$ one set of corresponding orbitals ($n\pi^*$) for which $\gamma = 1$, whereas $\gamma \approx 0$ for all other corresponding pairs. In this case eq 16 affords $\Delta\rho^{(\infty)} = \pi^*(1)\pi^*(1) - n(1)n(1')$, where we have made use of eq 17. The related excitation energy of eq 18 gives

$$\begin{aligned} \Delta E_{n \rightarrow \pi^*}^{(\infty)} &= E^{KS}[\pi^* \bar{n}] - E^{KS}[n \bar{n}] \\ &= \varepsilon_{\pi^*} - \varepsilon_n + 1/2K_{m, m} + 1/2K_{\pi^* \pi^*, \pi^* \pi^*} - K_{m, \pi^* \pi^*} \end{aligned} \quad (20)$$

where $E^{KS}[n \bar{n}]$ and $E^{KS}[\pi^* \bar{n}]$ are the KS energies of the ground-state determinant $|n \bar{n}|$ and excited-state determinant $|\pi^* \bar{n}|$, respectively. For the singlet excitation energy corresponding to $\Psi_{n \rightarrow \pi^*}^S = 1/(2)^{1/2} [|n \bar{\pi}^*| + |\pi^* \bar{n}|]$, use can be made of the Slater sum rules²⁴ to obtain

$$\begin{aligned} \Delta E_S^{(\infty)} &= 2E^{KS}[n \bar{\pi}^*] - E^{KS}[n \pi^*] - E^{KS}[n \bar{n}] \\ &= 2\Delta E_{n \rightarrow \pi^*}^{(\infty)} - \Delta E_{n \rightarrow \pi^*}^{(\infty)} \end{aligned} \quad (21)$$

We thus get from eq 20 and the corresponding expression for $E_{n \rightarrow \pi^*}^{(\infty)}$ that

$$\begin{aligned} \Delta E_S^{(\infty)} &= \varepsilon_{\pi^*} - \varepsilon_n + 1/2K_{m, m} + 1/2K_{\pi^* \pi^*, \pi^* \pi^*} \\ &\quad + 2K_{m, \pi^* \pi^*} - K_{m, \pi^* \pi^*} \end{aligned} \quad (22)$$

The expression for $\Delta E_S^{(2)}$ of eq 19 appears to be quite different from $\Delta E_S^{(\infty)}$ of eq 22. However, we note that if use is made of pure Hartree–Fock exchange then $K_{\pi^* \pi^*, \pi^* \pi^*}^{HF} = K_{m, m}^{HF} = 0$, whereas $K_{m, \pi^* \pi^*}^{HF} = -K_{\pi^* \pi^*, m}^{HF}$ and $K_{m, \pi^* \pi^*}^{HF} = -K_{\pi^* \pi^*, m}^{HF}$. Thus, in this case $\Delta E_S^{(2)HF} = \Delta E_S^{(\infty)HF}$. As a consequence, for Hartree–Fock the excitation energy of a single orbital transition is fully determined by $\Delta E_S^{(2)HF}$, and higher-order terms are zero. However, this is not the case for LDA, where $K_{\pi^* \pi^*, \pi^* \pi^*}^{LDA} \neq K_{m, m}^{LDA} \neq 0$, whereas $K_{m, \pi^* \pi^*}^{LDA} \neq -K_{\pi^* \pi^*, m}^{LDA}$ and $K_{m, \pi^* \pi^*}^{LDA} \neq -K_{\pi^* \pi^*, m}^{LDA}$. In this case the calculated excitation energies

are quite different depending on whether $\Delta E_S^{(2)}$ or $\Delta E_S^{(\infty)}$ is used. This is also the case for functionals based on the GGA.

The calculated singlet energies $\Delta E_S^{(\infty)LDA}$ are plotted in Figure 2 relative to the BE.¹⁰ It follows from the figure that CV(∞)-DFT in general affords too high excitation energies with a rmsd of 1.69 eV. This is opposite to CV(2)-DFT, where $\Delta E_S^{(2)LDA}$ systematically was too low. The contributions in eq 22 responsible for the high excitation energies are $K_{\pi^* \pi^*, \pi^* \pi^*}^{LDA}$ and especially $K_{m, m}^{LDA}$ which are both positive as the Coulomb contributions $K_{\pi^* \pi^*, \pi^* \pi^*}^C$, $K_{m, m}^C$ in absolute terms and are larger than the exchange contributions $K_{\pi^* \pi^*, \pi^* \pi^*}^{XC(LDA)}$, $K_{m, m}^{XC(LDA)}$. The lack of cancellation between Coulomb and exchange terms has been termed “self-interaction error” because the cancellation must be complete for a one-electron system. However, cancellation is not required to apply for many-electron systems where the term self-interaction error might be a misnomer.

It is perhaps not surprising that $\Delta E_S^{(\infty)LDA}$ is too high when we note in eq 20 that the orbital set used is optimized with respect to the ground state $|n \bar{n}|$ but not with respect to $|n \pi^*|$ and $|\pi^* \bar{n}|$. A more balanced description would result if the orbital sets were optimized separately for the ground state and each excited state, as suggested in the SCF-CV(∞)-DFT theory.²⁰ Such an optimization becomes especially simple for one-orbital excitations, such as $n \rightarrow \pi^*$, where we can employ the ΔSCF procedure^{24,30} and write

$$\Delta E_S^{(\Delta SCF)} = 2E_{SCF}^{KS}[n \bar{\pi}^*] - E_{SCF}^{KS}[n \pi^*] - E_{SCF}^{KS}[n \bar{n}] \quad (23)$$

In eq 23 $E_{SCF}^{KS}[n \bar{\pi}^*]$, $E_{SCF}^{KS}[n \pi^*]$ are the energies from SCF KS calculations on the configurations $n \bar{\pi}^*$ and $n \pi^*$, respectively, whereas $E_{SCF}^{KS}[n \bar{n}]$ is the SCF KS ground-state energy. We plot in Figure 2 $\Delta E_S^{(\Delta SCF)LDA}$ relative to BE.¹⁰ It is apparent that $\Delta E_S^{(\Delta SCF)LDA}$ represents a clear improvement over $\Delta E_S^{(2)LDA}$ and especially $\Delta E_S^{(\infty)LDA}$, with a rmsd of 0.54. It is interesting to note that $\Delta E_S^{(\Delta SCF)LDA}$ gives rise to a considerable lowering in energy compared to $\Delta E_S^{(\infty)LDA}$ for those cases (1, 2, and 10–15 of Figure 1), where $\Delta E_S^{(\infty)LDA}$ is much too high, whereas $\Delta E_S^{(\Delta SCF)LDA}$ hardly changes compared to $\Delta E_S^{(\infty)LDA}$ in those cases (3, 6, and 9 of Figure 1), where $\Delta E_S^{(\infty)LDA}$ is close to BE. Obviously for the pure functional LDA the ΔSCF procedure^{24,30} is the more accurate procedure. We note further that (1, 2, and

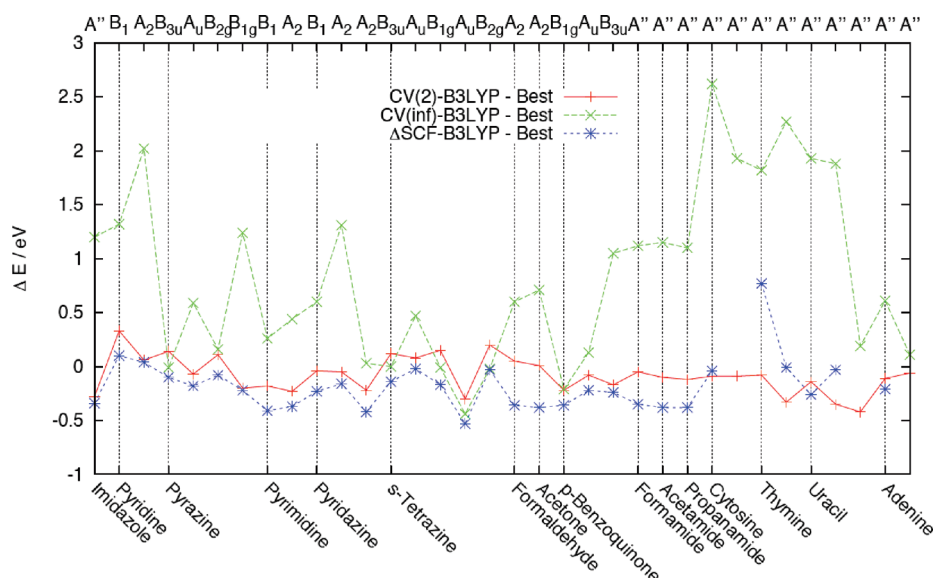


Figure 3. Difference between CV(2)-B3LYP, CV(∞)-B3LYP, ΔSCF-B3LYP, and BE.¹⁰

10–15) correspond to systems where n is localized on a single heteroatom leading to high values for $K_{nn,nn}^{LDA}$ whereas n in (3, 6, and 9) is delocalized over two or more heteroatoms resulting in much smaller values for $K_{nn,nn}^{LDA}$.

B3LYP. The B3LYP excitation energies are all given in Table 1. We plot further the calculated excitation energies due to CV(2)-DFT, CV(∞)-DFT, and ΔSCF relative to BE¹⁰ in Figure 3. It is to be noted that $\Delta E_S^{(2)B3LYP}$ for the various molecules is of a higher energy than $\Delta E_S^{(2)LDA}$. It is further in much better agreement with BE¹⁰ affording a rmsd of only 0.18 eV, Table 1. We attribute the increase in $\Delta E_S^{(2)B3LYP}$ compared to $\Delta E_S^{(2)LDA}$ to the larger gap in $\varepsilon_{\pi^*} - \varepsilon_n$ introduced by the 20% exact HF-exchange that is part of the B3LYP functional. We have in the evaluation of $\Delta E_S^{(2)B3LYP}$ according to eq 19 employed the Tamm–Dancoff approximation.²¹ Without this approximation one¹⁰ obtains quite similar results with rmsd of 0.22 eV. For CV(∞)-DFT we find again that the calculated excitation energies $\Delta E_S^{(\infty)}$ are larger than for that of $\Delta E_S^{(2)}$. This is especially the case for those systems (1, 2, and 10–15), where n is located on a single heteroatom (N or O). However compared to LDA, the difference $\Delta E_S^{(2)} - \Delta E_S^{(\infty)}$ has decreased in the case of B3LYP, and the rmsd is now 1.14 eV, Table 1. The reductions stem from the fact that the 20% HF-exchange in B3LYP do not contribute to $\Delta E_S^{(2)} - \Delta E_S^{(\infty)}$ as argued previously. Introducing finally ΔSCF leads, as in the case of LDA, to a considerable improvement with a rmsd of 0.30 eV, which is only slightly larger than for $\Delta E_S^{(2)B3LYP}$ with rmsd of 0.18 eV. For the $n \rightarrow \pi^*$ transitions studied here, the B3LYP proves to afford excitation energies closest to BE¹⁰ for both $\Delta E_S^{(2)}$ and $\Delta E_S^{(\infty)}$. Unfortunately, in a few cases we were unable to obtain SCF convergence for the ΔSCF method. These cases are marked by blank entries in Table 1.

GGA, MO6-L, BHLYP, and MO6. Exploratory calculations with standard functionals based on the GGA revealed that that these functionals afford results quite similar in quality to LDA. A possible exception is the meta-GGA functional MO6-L,^{34,35} which has been applied by Jacquemin et al. for the same sample of excitation shown in Table 1 yielding a rmsd of 0.45 eV. We have also carried out a full investigation employing the BHLYP functional with 50% HF exchange. The results are not reported in details as they follow the same trends as B3LYP. Thus, for CV(2)-

DFT the excitation energies are somewhat overestimated with a rmsd of 0.69 eV using the Tamm–Dancoff approximation²¹ and 0.62 eV without.¹⁰ Introducing CV(∞)-DFT increases the excitation energies even more with a rmsd of 0.93 eV. Finally relaxing the orbitals in ΔSCF leads to a substantial improvement with a rmsd of 0.48 eV. It is apparent from the BHLYP results given in Table S1 of the Supporting Information that a considerable increase in the fraction of exact exchange in B3LYP from 20% leads to a poorer agreement with BE.¹⁰ We should note that the MO6 functional by Zhao and Truhlar⁸ with 27% HF-exchange for the sample of excitations in Table 1 affords a rmsd of 0.24 eV.

5. CONCLUDING REMARKS

We have carried out a theoretical study of $n \rightarrow \pi^*$ transitions based on constricted variational density functional theory (CV(n)-DFT)^{18,20} as a natural extension of a previous study on $\pi_A \rightarrow \pi_B^*$ CT transitions.¹⁵ In both types of excitations an electron is moved between two regions of space with little overlap where the regions are defined by the density of the orbitals involved. In CV(n)-DFT we carry out a unitary transformation $\exp[U]$ of eq 1 between the occupied $\{\varphi_i; i = 1, \text{occ}\}$ and virtual $\{\varphi_a; a = 1, \text{vir}\}$ ground-state orbitals to any desired order n in U to produce a new set of occupied $\{\varphi'_i; i = 1, \text{occ}\}$ and virtual $\{\varphi'_a; a = 1, \text{vir}\}$ excited state orbitals.²⁰ Here the matrix U consists of $\text{occ} \times \text{vir}$ independent variational parameters that are determined in such a way as to minimize the excitation energies under the constraint that the change in density due to an excitation represents the transfer of one electron from the density space spanned by $\{\varphi_i; i = 1, \text{occ}\}$ to the density space spanned by $\{\varphi_a; a = 1, \text{vir}\}$.^{18,20}

For the CV(2)-DFT level of theory we recover within the Tamm–Dancoff approximation²¹ the adiabatic TDDFT theory^{1,2} of eq 14. It was shown in our previous study on $\pi_A \rightarrow \pi_B^*$ CT transitions¹⁵ that the energy expression ($\Delta E_S^{(2)}$) for CV(2)-DFT or adiabatic TDDFT is unable even qualitatively to describe CT transition energies. Further, for such transitions, $\Delta E_S^{(2)}$ leads to a severe underestimation of the excitation energies. In the case of the $n \rightarrow \pi^*$ type of transitions the error for $\Delta E_S^{(2)}$ is much smaller and

for B3LYP, we find that $\Delta E_S^{(2)B3LYP}$ is in close agreement with BE¹⁰ leading to a rmsd of only 0.18 eV.

For the CT transitions $\pi_A \rightarrow \pi_B^*$ the inclusion of energy terms to all orders in U (CV(∞)-DFT) leads to a qualitative correct energy expression $\Delta E_S^{(\infty)}$ which contains the “self-interaction” terms $K_{\pi_A \pi_A^* \pi_B \pi_B^*}$, $K_{\pi_B \pi_B^* \pi_A \pi_A^*}$. Further, combining the energy expression $\Delta E_S^{(\infty)}$ with a relaxation of $\{\varphi_i; i = 1, \text{occ}\}$ and $\{\varphi_a; a = 1, \text{vir}\}$ gives rise to excitation energies ($\Delta E_S^{(\Delta SCF)}$) in excellent agreement with experiment even for LDA where the rmsd was 0.20 eV [15]. In the case of $n \rightarrow \pi^*$ transitions, the inclusion of terms to all orders followed by orbital relaxation as accomplished in the ΔSCF procedure^{24,30} results for LDA and B3LYP in a better agreement with BE¹⁰ than $\Delta E_S^{(2)}$. However, for B3LYP $\Delta E_S^{(2)}$ and $\Delta E_S^{(\Delta SCF)}$ are quite close with rmsd values of 0.18 and 0.30 eV, respectively. The orbital relaxation achieves in many ways the same as the introduction of double displacements through frequency dependent kernels.³¹

The $n \rightarrow \pi^*$ transitions discussed here are of a special kind that can be described by a single orbital transition. This considerably simplifies the self-consistent optimization of U through the use of the ΔSCF procedure.^{24,30} For the general transition involving many orbital transitions the self-consistent optimization of U has been formulated but not yet implemented.²⁰ We finally note that we have modified the name of our approach from constrained variational theory in the previous study¹⁵ to constricted variational theory in the present investigation. This is done in order not to confuse our CV(n)-DFT approach with other constrained variational methods in the literature.^{32,33} In the method by Van Voorhis,³² charge is constrained to certain regions of Cartesian space, whereas our method constricts the charge to certain regions of orbital space.

■ ASSOCIATED CONTENT

Supporting Information. Results from B3LYP functional given in Table S1. This material is available free of charge via the Internet at <http://pubs.acs.org>.

■ AUTHOR INFORMATION

Corresponding Author

*E-mail: ziegler@ucalgary.ca.

■ ACKNOWLEDGMENT

T.Z. would like to thank the Canadian government for a Canada research chair in theoretical inorganic chemistry and the NSERC for financial support. J.C. would like to thank University of Manitoba for a sabbatical leave.

■ REFERENCES

- (1) Runge, E.; Gross, E. K. U. *Phys. Rev. Lett.* **1984**, 52, 997.
- (2) Casida, M. E. In *Recent advances in density functional methods*; Chong, D. P., Ed.; World Scientific: Singapore, 1995; pp 155–193.
- (3) van Gisbergen, S. J. A.; Snijders, J. G. *J. Chem. Phys.* **1995**, 103, 9347.
- (4) Petersilka, M.; Grossmann, U. J.; Gross, E. K. U. *Phys. Rev. Lett.* **1996**, 76, 12.
- (5) Bauernschmitt, R.; Ahlrichs, R. *Chem. Phys. Lett.* **1996**, 256, 454.
- (6) Stratmann, R. E.; Scuseria, G. E.; Frisch, M. J. *J. Chem. Phys.* **1998**, 109, 8218.
- (7) Jensen, F. *Introduction to Computational Chemistry*; Wiley: New York, 2006.
- (8) Jacquemin, D.; Perpète, E. A.; Ciofini, I.; Adamo, C.; Valero, R.; Zhao, Y.; Truhlar, D. G. *J. Chem. Theory Comput.* **2010**, 6, 2071.

- (9) Goerigk, L.; Grimme, S. *J. Chem. Phys.* **2010**, 132, 184103.
- (10) Schreiber, M.; Silva-Junior, M.; Sauer, S.; Thiel, W. *J. Chem. Phys.* **2008**, 128, 134110.
- (11) (a) Tawada, Y.; Tsuneda, T.; Yanagisawa, S.; Yanai, T.; Hirao, K. *J. Phys. Chem.* **2004**, 120, 8425. (b) Song, J.-W.; Watson, M. A.; Hirao, K. *J. Chem. Phys.* **2009**, 131, 144108.
- (12) Stein, T.; Kronik, L.; Baer, R. *J. Am. Chem. Soc.* **2009**, 131, 2818.
- (13) (a) Neugebauer, J.; Gritsenko, O.; Baerends, E. J. *J. Chem. Phys.* **2006**, 124, 214102. (b) Schipper, P. R. T.; Gritsenko, O. V.; van Gisbergen, S. J. A.; Baerends, E. J. *J. Chem. Phys.* **2000**, 112, 1344–1352.
- (14) Gritsenko, O.; Baerends, E. J. *J. Chem. Phys.* **2004**, 121, 655–660.
- (15) Ziegler, T.; Krykunov, M. *J. Chem. Phys.* **2010**, 133, 074104.
- (16) Ziegler, T.; Seth, M.; Krykunov, M.; Autschbach, J.; Wang, F. *J. Mol. Struct. THEOCHEM* **2009**, 914, 106.
- (17) Ziegler, T.; Seth, M.; Krykunov, M.; Autschbach, J. *J. Chem. Phys.* **2008**, 129, 184114.
- (18) Ziegler, T.; Seth, M.; Krykunov, M.; Autschbach, J.; Wang, F. *Chem. Phys.* **2009**, 130, 154102.
- (19) Zhao, Y.; Truhlar, D. G. *J. Phys. Chem.* **2008**, A 112, 1095.
- (20) Cullen, J.; Krykunov, M.; Ziegler, T. *Chem. Phys.*, in press, doi:10.1016/j.chemphys.2011.05.021.
- (21) Hirata, S.; Head-Gordon Chem, M. *Phys. Lett.* **1999**, 314, 291.
- (22) Vosko, S. H.; Wilk, L.; Nusair, M. *Can. J. Phys.* **1980**, 58, 1200.
- (23) Becke, A. D. *J. Chem. Phys.* **1993**, 98, 5648.
- (24) Ziegler, T.; Baerends, E. J.; Rauk, A. *Theoret. Chim. Acta (Berlin)* **1976**, 43, 261.
- (25) te Velde, G.; Bickelhaupt, F. M.; van Gisbergen, S. J. A.; Fonseca Guerra, C.; Baerends, E. J.; Snijders, J. G.; Ziegler, T. *J. Comput. Chem.* **2001**, 22, 931.
- (26) Van Lenthe, E.; Baerends, E. J. *J. Comput. Chem.* **2003**, 24, 1142.
- (27) Amos, A. T.; Hall, G. G. *Proc. R. Soc.* **1961**, A263, 483.
- (28) Martin, R. L. *J. Chem. Phys.* **2003**, 118, 4775.
- (29) Ziegler, T.; Rauk Theoret, A. *Chim. Acta (Berlin)* **1977**, 46, 1.
- (30) Slater, J. C.; Johnson, K. H. *Phys. Rev. B* **1972**, 844–853.
- (31) Maitra, N. T.; Zhang, F.; Cave, R. J.; Burke, R. *J. Chem. Phys.* **2004**, 120, 5932.
- (32) (a) Cheng, C. L.; Wu, Q.; Van Voorhis, T. *J. Chem. Phys.* **2008**, 129, 124112. (b) Wu, Q.; Van Voorhis, T. *Phys. Rev. A* **2005**, 72 (2), 024502.
- (33) Artacho, E.; Rohlfling, M.; Côté, M.; Haynes, P. D.; Needs, R. J.; Molteni, C. *Phys. Rev. Lett.* **2004**, 93, 116401.
- (34) Zhao, Y.; Truhlar, D. G. *J. Chem. Phys.* **2006**, 125, 194101.
- (35) Zhao, Y.; Truhlar Theor, D. G. *Chem. Acc.* **2008**, 120, 215.